Differential impact of *Ink4a* and *Arf* on hematopoietic stem cells and their bone marrow microenvironment in *Bmi1*-deficient mice

Hideyuki Oguro,[1,2] Atsushi Iwama,[2] Yohei Morita,[1] Takehiko Kamijo,[3] Maarten van Lohuizen,[4] and Hiromitsu Nakauchi[1]

[1]Laboratory of Stem Cell Therapy, Center for Experimental Medicine, Institute of Medical Sciences, University of Tokyo, Tokyo 108-8679, Japan
[2]Department of Cellular and Molecular Medicine, Graduate School of Medicine, Chiba University, Chiba 260-8670, Japan
[3]Division of Biochemistry, Chiba Cancer Center Research Institute, Chiba 260-8717, Japan
[4]Division of Molecular Genetics, The Netherlands Cancer Institute, 1066 CX Amsterdam, Netherlands

The polycomb group (PcG) protein Bmi1 plays an essential role in the self-renewal of hematopoietic and neural stem cells. Derepression of the *Ink4a/Arf* gene locus has been largely attributed to *Bmi1*-deficient phenotypes in the nervous system. However, its role in hematopoietic stem cell (HSC) self-renewal remained undetermined. In this study, we show that derepressed $p16^{Ink4a}$ and $p19^{Arf}$ in *Bmi1*-deficient mice were tightly associated with a loss of self-renewing HSCs. The deletion of both *Ink4a* and *Arf* genes substantially restored the self-renewal capacity of $Bmi1^{-/-}$ HSCs. Thus, Bmi1 regulates HSCs by acting as a critical failsafe against the $p16^{Ink4a}$- and $p19^{Arf}$-dependent premature loss of HSCs. We further identified a novel role for Bmi1 in the organization of a functional bone marrow (BM) microenvironment. The BM microenvironment in $Bmi1^{-/-}$ mice appeared severely defective in supporting hematopoiesis. The deletion of both *Ink4a* and *Arf* genes did not considerably restore the impaired BM microenvironment, leading to a sustained postnatal HSC depletion in $Bmi1^{-/-}Ink4a\text{-}Arf^{-/-}$ mice. Our findings unveil a differential role of derepressed *Ink4a* and *Arf* on HSCs and their BM microenvironment in *Bmi1*-deficient mice. Collectively, Bmi1 regulates self-renewing HSCs in both cell-autonomous and nonautonomous manners.

CORRESPONDENCE
Atsushi Iwama:
aiwama@faculty.chiba-u.jp
OR
Hiromitsu Nakauchi:
nakauchi@ims.u-tokyo.ac.jp

Polycomb group (*PcG*) genes are involved in cellular memory by maintaining gene silencing through chromatin modifications (1, 2). Recent studies have implicated the role of *PcG* genes in stem cell self-renewal, a process in which cellular memory is precisely maintained through cell division (2, 3). Among *PcG* genes, *Bmi1* plays a central role in the inheritance of the stemness of hematopoietic and neural stem cells (3–8), and its forced expression promotes hematopoietic stem cell (HSC) self-renewal (8). These findings highlight the importance of epigenetic regulation in stem cell self-renewal.

One of the major Bmi1 targets is the *Ink4a/Arf* locus (9). This locus encodes a cyclin-dependent kinase inhibitor, $p16^{Ink4a}$, and a tumor suppressor, $p19^{Arf}$. $p16^{Ink4a}$ inhibits the binding of cyclin D to Cdk4/6 and keeps retinoblastoma protein (Rb) hypophosphorylated. Hypophosphorylated Rb represses E2F-dependent transcription by sequestrating E2F, ultimately leading to cell cycle arrest or senescence. $p19^{Arf}$ inhibits MDM2 and ARF-BP1, which mediate the ubiquitin-dependent degradation of p53, leading to the accumulation of p53 protein. This results in activation of the p53 target genes involved in cell cycle arrest, apoptosis, or senescence (10). In *Bmi1*-deficient mice, the expression of *Ink4a* and *Arf* is markedly increased in hematopoietic cells (7, 8), and the enforced expression of *Ink4a* and *Arf* in HSCs resulted in cell cycle arrest and p53-dependent apoptosis, respectively (7). Conversely, *Bmi1*;*Ink4a/Arf* compound mutant mice (hereafter referred to as $Bmi1^{-/-}Ink4a\text{-}Arf^{-/-}$ mice) exhibited a substantial recovery

The online version of this article contains supplemental material.

of hematopoietic cells, as indicated by restored lymphocyte counts (9, 11), as well as of the self-renewal capacity of neural stem cells (11, 12). However, the real impact of derepressed *Ink4a* and *Arf* in self-renewing HSCs has not yet been determined using a genetic approach.

To address this question, we performed a detailed analysis of HSCs in *Bmi1*$^{-/-}$*Ink4a-Arf*$^{-/-}$ mice and identified a critical role for Bmi1-dependent repression of the p16^{Ink4a}–Rb and p19^{Arf}–p53 pathways in the maintenance of self-renewing HSCs. We further demonstrated evidence of the involvement of Bmi1 in the regulation of HSCs and their BM microenvironment in a way that is not associated with the *Ink4a* and *Arf* locus.

RESULTS AND DISCUSSION

To clarify the contribution of derepressed *Ink4a* and *Arf* to the self-renewal defect of *Bmi1*$^{-/-}$ HSCs, we evaluated the competitive repopulation capacity of *Bmi1*$^{-/-}$*Ink4a-Arf*$^{-/-}$ HSCs. Total BM cells from 4-wk-old wild-type, *Ink4a-Arf*$^{-/-}$, *Bmi1*$^{-/-}$, and *Bmi1*$^{-/-}$*Ink4a-Arf*$^{-/-}$ mice (C57BL/6-Ly5.2) were infused into lethally irradiated recipients (C57BL/6-Ly5.1) along with the same number of competitor BM cells from C57BL/6-Ly5.1 mice. *Bmi1*$^{-/-}$*Ink4a-Arf*$^{-/-}$ BM cells exhibited a mostly normal long-term repopulating activity of the recipient BM in both primary and secondary transplantations, whereas *Bmi1*$^{-/-}$ BM cells did not contribute to long-term repopulation at all (Fig. 1, A and B). *Bmi1*$^{-/-}$*Ink4a-Arf*$^{-/-}$ BM cells fully repopulated recipients' BM in cellularity (Fig. 1 C) and also manifested a full differentiation capacity along myeloid and lymphoid lineages (Fig. 1 D). As evident in Fig. S1 (available at http://www.jem.org/cgi/content/full/jem.20052477/DC1), the frequencies of *Bmi1*$^{-/-}$ and *Bmi1*$^{-/-}$*Ink4a-Arf*$^{-/-}$ CD34^{-}c-Kit^{+}Sca-1^{+}lineage marker^{-} (KSL) cells, which are highly enriched for long-term repopulating HSCs (13), were comparable with that of the wild type. *Bmi1*$^{-/-}$ mice displayed a HSC frequency no less than that of the wild type, and *Bmi1*$^{-/-}$*Ink4a-Arf*$^{-/-}$ mice exhibited almost the same HSC frequency as that of the wild type. Thus, the number of HSCs infused was comparable among recipients in the competitive repopulation assay. Even with 10 times more donor cells, *Bmi1*$^{-/-}$ BM cells did not contribute to the repopulation at all, highlighting a severe defect of *Bmi1*$^{-/-}$ HSC function (Fig. S2). All of these data clearly demonstrate that the defective self-renewal capacity of *Bmi1*$^{-/-}$ HSCs could be substantially rescued by the deletion of *Ink4a* and *Arf*, thus defining the *Ink4a/Arf* locus as a critical Bmi1 target for the maintenance of HSC self-renewal.

The deletion of *Arf* alone scarcely restored the self-renewal defect of *Bmi1*$^{-/-}$ HSCs, and the chimerism of *Bmi1*$^{-/-}$*Arf*$^{-/-}$ hematopoietic cells in peripheral blood gradually decreased with time (unpublished data). This presents a striking contrast to the major role of *Arf* derepression in *Bmi1*$^{-/-}$ phenotypes in neural stem cell self-renewal and cerebellar granule neuron progenitor proliferation (11).

To further evaluate the proliferative and differentiation capacity of *Bmi1*$^{-/-}$*Ink4a-Arf*$^{-/-}$ HSCs, we purified the CD34^{-}KSL HSC fraction, and an in vitro single-cell culture was performed for 14 d in the presence of stem cell factor (SCF), IL-3, thrombopoietin (TPO), and erythropoietin (EPO). Although *Bmi1*$^{-/-}$ HSCs contained 3.3-fold fewer high proliferative potential (HPP) colony-forming cells (CFCs) than the wild type, *Bmi1*$^{-/-}$*Ink4a-Arf*$^{-/-}$ HSCs contained a comparable number of HPP-CFCs with the wild type (Fig. 2 A). We have previously demonstrated that CFU-neutrophil/macrophage/erythroblast/megakaryocyte (nmEM), which retains multilineage differentiation capacity, is a major subpopulation among CD34^{-}KSL HSCs but

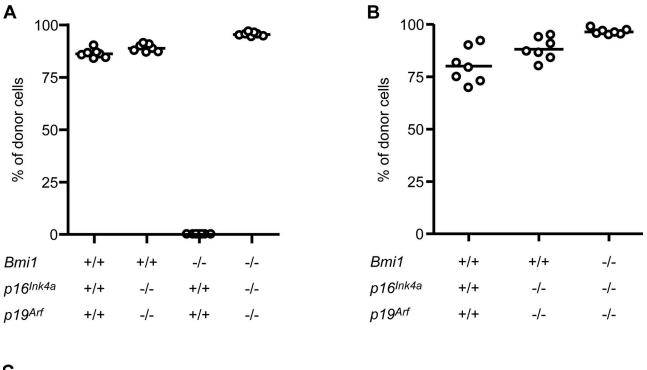

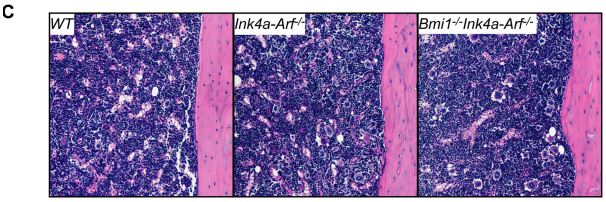

D

Mice	Percent chimerism			
	All WBCs	Myeloid	T lymphoid	B lymphoid
WT	86.1±2.06	85.8±4.12	73.6±1.83	91.9±2.21
Ink4a-Arf$^{-/-}$	88.8±1.78	89.5±2.07	78.9±5.54	92.0±2.72
Bmi1$^{-/-}$	0±0	0±0	0±0	0±0
Bmi1$^{-/-}$*Ink4a-Arf*$^{-/-}$	95.4±0.92	98.6±0.38	76.5±4.98	98.8±0.30

Figure 1. Substantial recovery of the defective repopulation capacity of *Bmi1*$^{-/-}$ HSCs by the deletion of *Ink4a* and *Arf*. (A) Competitive lymphohematopoietic repopulating assay. 1 × 10^6 pooled test BM cells from 4-wk-old mice (B6-Ly5.2) were mixed with 1 × 10^6 competitor BM cells from 12-wk-old wild-type mice (B6-Ly5.1) and injected into lethally irradiated recipient mice (B6-Ly5.1; $n = 7$). The percent chimerism of donor cells in the recipient peripheral blood cells 12 wk after transplantation is presented. (B) Secondary transplantation analysis. 2 × 10^6 pooled BM cells from primary recipients were injected into lethally irradiated secondary recipient mice (B6-Ly5.1; $n = 7$). The percent chimerism of donor cells 12 wk after transplantation is presented. (A and B) The mean values are indicated as horizontal bars. (C) Hematoxylin and eosin staining of sections of decalcified femur from primary recipients that had transplanted donor cells of the indicated genotype 12 wk before. Donor cell chimerism in the recipient peripheral blood cells was around 90%, as depicted in A and D, and the absolute BM cell numbers were comparable (4.2 × 10^7 *WT* cells, 4.75 × 10^7 *Ink4a-Arf*$^{-/-}$ cells, and 4.15 × 10^7 *Bmi1*$^{-/-}$*Ink4a-Arf*$^{-/-}$ cells for one pair of femur and tibia). (D) The percent chimerism of donor cells in each lineage 12 wk after primary transplantation is presented as the mean ± SD. WBC, white blood cell.

not among $CD34^+KSL$ multipotential progenitor cells and that its frequency is well correlated with that of functional HSCs (14). Of note, the morphological analysis of HPP colonies revealed that *Bmi1*$^{-/-}$ $CD34^-KSL$ cells present a drastic reduction in their frequency of CFU-nmEM, whereas *Bmi1*$^{-/-}$*Ink4a-Arf*$^{-/-}$ HSCs show a substantial recovery in their frequency of CFU-nmEM compared with the wild type (Fig. 2 B). In an in vitro culture of pooled $CD34^-KSL$ HSCs, however, *Bmi1*$^{-/-}$*Ink4a-Arf*$^{-/-}$ HSCs exhibited a considerable but only partial recovery of proliferation (Fig. 2 C). In vitro culture systems are a kind of stringent condition in which numerous signaling entities are missing that are supportive for HSCs and are present in the in vivo microenvironment. Thus, these findings suggest that the deletion of *Ink4a* and *Arf* does not completely restore the defective proliferative and differentiation capacity of *Bmi1*$^{-/-}$ HSCs.

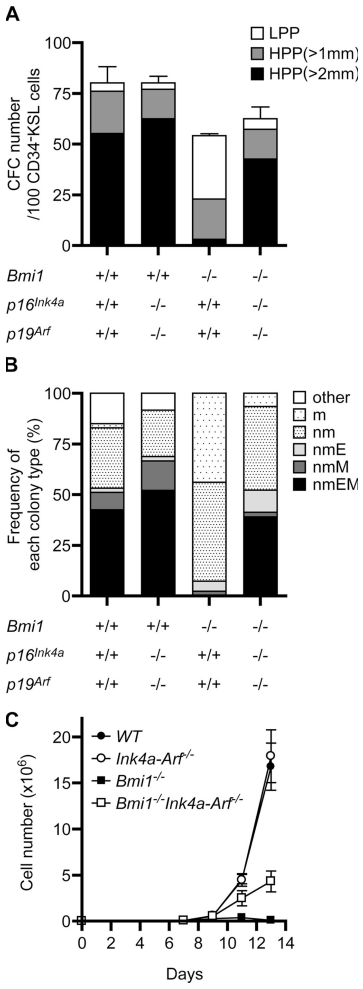

Figure 2. The deletion of *Ink4a* and *Arf* largely restores the proliferative and differentiation capacity of *Bmi1*$^{-/-}$ HSCs in vitro. (A) Single HSC growth assay. 96 individual $CD34^-KSL$ HSCs were sorted clonally into 96-well microtiter plates in the presence of SCF, IL-3, TPO, and EPO. The numbers of high (HPP) and low proliferative potential (LPP) CFCs were retrospectively evaluated by counting colonies on day 14 (HPP- and LPP-CFCs, colony diameters of >1 and <1 mm, respectively). The results are shown as the mean ± SD (error bars) of triplicate cultures. (B) Frequency of each colony type. Colonies derived from HPP-CFCs were recovered and morphologically identified as neutrophils (n), macrophages (m), erythroblasts (E), or megakaryocytes (M). (C) Growth of $CD34^-KSL$ HSCs in vitro. 50 freshly isolated $CD34^-KSL$ cells were cultured in the presence of SCF, IL-3, and TPO. The results are shown as the mean ± SD of triplicate cultures.

We next examined hematopoiesis in *Bmi1*$^{-/-}$*Ink4a-Arf*$^{-/-}$ mice in detail. The peripheral leukocyte count of *Bmi1*$^{-/-}$*Ink4a-Arf*$^{-/-}$ mice recovered to the same level as that of the wild type (Fig. 3 A). However, the recovery of BM cellularity as well as the number of $CD34^-KSL$ HSCs was incomplete in *Bmi1*$^{-/-}$*Ink4a-Arf*$^{-/-}$ mice, and, unexpectedly, their numbers progressively decreased over time (Fig. 3, B and C). Histological analysis of femurs showed a severely hypoplastic fatty marrow in *Bmi1*$^{-/-}$ mice as previously described (4). This phenotype was not completely rescued by the deletion of *Ink4a* and *Arf* genes and severely progressed even in *Bmi1*$^{-/-}$*Ink4a-Arf*$^{-/-}$ mice (Fig. 3 D). Given that the BM repopulation capacity of *Bmi1*$^{-/-}$*Ink4a-Arf*$^{-/-}$ HSCs is mostly normal (Fig. 1, A and B), these data indicate defects of the BM microenvironment in the absence of Bmi1. This possibility was confirmed by transplanting wild-type BM cells into irradiated *Bmi1*$^{-/-}$ mice. Although the peripheral blood leukocyte count and the spleen weight in *Bmi1*$^{-/-}$ recipients recovered to the wild-type level after transplantation, the histological analysis of recipients' femurs and their BM cell counts demonstrated that the *Bmi1*$^{-/-}$ BM microenvironment is defective in supporting the BM repopulation by wild-type HSCs (Fig. 4, A–D). Surprisingly, the deletion of both *Ink4a* and *Arf* did not considerably restore the impaired capacity of the *Bmi1*$^{-/-}$ BM microenvironment to support hematopoiesis by wild-type HSCs (Fig. 4, A and C).

The regulation of self-renewal and differentiation of HSCs requires a specific BM microenvironment. In BM, a subpopulation of osteoblasts has been implicated as an important component of the HSC niche, indicating that the bone surface is the major HSC niche (15–17). The size of the osteoblastic niche is largely dependent on the amount of trabecular bone (15, 16). In *Bmi1*$^{-/-}$ BM, development of the trabecular bone was severely impaired, particularly in the metaphyseal area (Fig. 4 E). This indicates a profound reduction in the osteoblastic niche and raises the possibility of an insufficient production of osteoblasts.

To further characterize the role of Bmi1 in osteoblasts as niche cells, we analyzed primary cultured *Bmi1*$^{-/-}$ osteoblasts. *Bmi1*$^{-/-}$ osteoblasts showed a normal level of alkaline phosphatase activity, which is one of the representative osteoblastic differentiation markers (Fig. S3 A, available at http://www.jem.org/cgi/content/full/jem.20052477/DC1). RT-PCR analysis of the osteoblast-specific marker genes (*Osteopontin*, *Osteocalcin*, *Runx2*, *Ostetix*, and *Col1a1*) as well as known HSC niche factor genes (*N-cadherin*, *Angiopoietin-1*, *-2*, *Jagged-1*, and *SCF*) was unable to discern any gross difference between the wild-type and *Bmi1*$^{-/-}$ osteoblasts, although *p16*^{Ink4a} and *p19*^{Arf} were also derepressed in

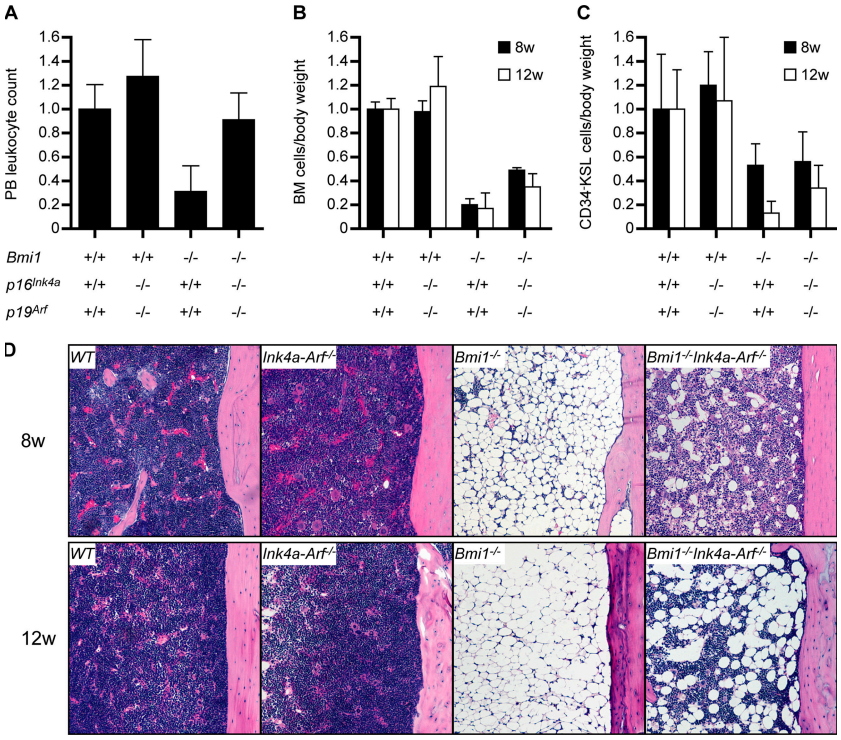

Figure 3. Incomplete recovery of defective hematopoiesis in *Bmi1*$^{-/-}$*Ink4a-Arf*$^{-/-}$ mice. (A) Peripheral blood leukocyte count in 8-wk-old mice ($n \geq 4$). (B) BM mononuclear cell count per body weight ($n \geq 3$). (C) Quantification of the number of CD34^{-}KSL cells per body weight ($n \geq 3$). All data were normalized relative to the wild type and are shown as the mean ± SD (error bars). (D) Hematoxylin and eosin staining of sections of decalcified femur from 8- and 12-wk-old mice.

Bmi1$^{-/-}$ osteoblasts (Fig. S3 B). We then took advantage of the *Bmi1* knockdown technique. Osteoblasts were infected with a lentivirus expressing short hairpin RNA (shRNA) against *Bmi1*, which efficiently inhibited the transcription of *Bmi1* (Fig. 4 F). Consistent with in vivo trabecular bone formation, *Bmi1* knockdown led to a reduced osteoblast proliferation (Fig. 4 F). Nonetheless, *Bmi1* knockdown osteoblasts similarly supported the survival and multilineage differentiation capacity of CD34^{-}KSL HSCs during a 5-d ex vivo culture (Fig. S3 C). Collectively, these findings suggest that Bmi1 controls the BM microenvironment, at least in part, by regulating osteoblast niche size. In contrast with the case of HSCs, however, the deletion of both *Ink4a* and *Arf* again did not substantially restore the impaired development of the trabecular bone (Fig. 4 E) or the impaired proliferation of *Bmi1* knockdown osteoblasts (Fig. 4 F), confirming that the *Ink4a* and *Arf* genes are not the major targets for Bmi1 in the maintenance of the BM microenvironment, as demonstrated in Fig. 4 (A and C). The BM microenvironment consists of not only osteoblasts but also stromal cells, endothelial cells (18), and so on. It would be intriguing to ask whether Bmi1 also functions in the other components of the BM microenvironment.

Our findings in this study clearly demonstrate that the derepression of *Ink4a* and *Arf* genes is responsible for defective HSC self-renewal. However, we have previously reported that *Bmi1*$^{-/-}$ HSCs undergo the first cell division in a fashion similar to that of the wild type and showed no apoptosis in a single HSC culture. In addition, cell cycle analysis of BM primitive hematopoietic cells (KSL and Lin^{-} cells) did not detect any difference between the wild-type and *Bmi1*$^{-/-}$ mice (8). These findings indicate that the derepression of *Ink4a* and *Arf* genes in *Bmi1*$^{-/-}$ mice do not grossly affect the cell cycle or survival of HSCs.

It has been well recognized that the activated p16^{Ink4a}–Rb and p19^{Arf}–p53 pathways are profoundly associated with cellular senescence (19). Cellular senescence is a program activated by normal cells in response to various types of stress. These include telomere attrition, DNA damage, oxidative stress, oncogenic stress, and others. Senescence of HSCs is supposed to be induced by telomere-dependent and -independent pathways (20, 21). We first measured the telomere length of wild-type and *Bmi1*$^{-/-}$ lineage marker^{-} immature cells and lineage marker^{+} differentiated cells by fluorescence in situ hybridization. The loss of *Bmi1* did not alter the telomere length at all (Fig. 5 A). In the absence of Bmi1, the derepression of *Ink4a* and *Arf* genes causes the premature senescence of mouse embryonic fibroblasts (9). *Bmi1* knockdown osteoblasts indeed exhibited a higher senescence-associated (SA) β-galactosidase activity, which was canceled in the absence of *Ink4a* and *Arf* genes (Fig. S4, available at http://www.jem.org/cgi/content/full/jem.20052477/DC1), suggesting that

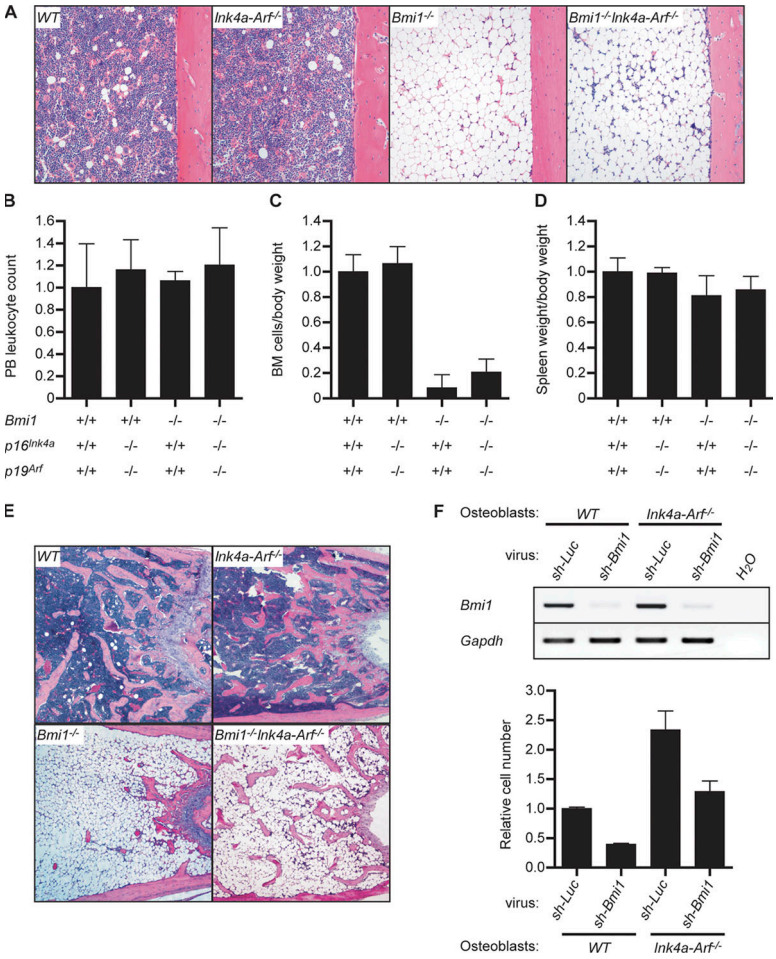

Figure 4. Impaired BM microenvironment in *Bmi1*$^{-/-}$ mice. (A–D) Wild-type, *Ink4a-Arf*$^{-/-}$, *Bmi1*$^{-/-}$, and *Bmi1*$^{-/-}$*Ink4a-Arf*$^{-/-}$ recipient mice were transplanted with 2×10^6 wild-type BM cells. At 4 wk after transplantation, recipient mice were analyzed on their BM cellularity (femur, A), peripheral blood leukocyte count (B), BM cell number per body weight (C), and spleen weight per body weight (D). Donor cell chimerism in recipient peripheral blood mononuclear cells was 80.1 ± 4.2, 78.7 ± 2.4, 98.8 ± 0.38, and 82.5 ± 10.1% with wild-type, *Ink4a-Arf*$^{-/-}$, *Bmi1*$^{-/-}$, and *Bmi1*$^{-/-}$*Ink4a-Arf*$^{-/-}$ recipients, respectively ($n \geq 3$). (E) Hematoxylin and eosin staining of sections of decalcified distal femur from 8-wk-old mice. (F) Analyses of *Bmi1* knockdown osteoblasts. Primary cultured wild-type and *Ink4a-Arf*$^{-/-}$ osteoblasts were infected with lentiviruses expressing shRNA against either *luciferase* (Luc; control) or *Bmi1*. The infection efficiency was almost 100% in all knockdown experiments. The knockdown efficiencies were evaluated by detecting *Bmi1* mRNA expression by RT-PCR analysis (top), and their growth was monitored at day 5 of culture (bottom). The results are shown as the mean ± SD (error bars) of triplicate cultures.

Bmi1 controls the cellular senescence of osteoblasts by regulating the expression of *Ink4a* and *Arf* genes. We then analyzed freshly isolated *Bmi1*$^{-/-}$ CD34$^-$KSL HSCs in terms of the SA–β-galactosidase activity and SA gene expression profiles, but all appeared negative (unpublished data). It is possible that the senescent HSCs do not express specific combinations of marker antigens for HSC identification any more. Thus, the possibility that derepressed *Ink4a* and *Arf* genes facilitate the premature senescence of HSCs remains to be determined.

In contrast to the strong impact of derepressed p16^{Ink4a} and p19^{Arf} on HSC self-renewal, the loss of p16^{Ink4a} and p19^{Arf} has been reported to have a limited role in this process (22). In our analyses, freshly isolated *Ink4a-Arf*$^{-/-}$HSCs did not show any advantages in competitive BM repopulation assays either. However, *Ink4a-Arf*$^{-/-}$ HSCs retained their self-renewal capacity better than the wild type during long-term ex vivo culture (unpublished data). These findings suggest that a tight repression of *Ink4a* and *Arf* genes by Bmi1 accounts for a positive effect of forced *Bmi1* expression on HSC self-renewal and multipotential progenitor expansion (8). To confirm this, we transduced *Ink4a-Arf*$^{-/-}$ HSCs with a *Bmi1* retrovirus, cultured for 10 d in the presence of SCF and TPO, and subjected the cells to colony assays. Unexpectedly, the overexpression of Bmi1 in *Ink4a-Arf*$^{-/-}$ HSCs again induced a similar mode of multipotential progenitor expansion to that in wild-type HSCs (Fig. 5 B). These data, together with the incomplete recovery in the proliferative capacity of *Bmi1*$^{-/-}$*Ink4a-Arf*$^{-/-}$ HSCs in vitro, indicate that additional targets for Bmi1 exist other than *Ink4a* and *Arf* genes, which are implicated in the regulation of

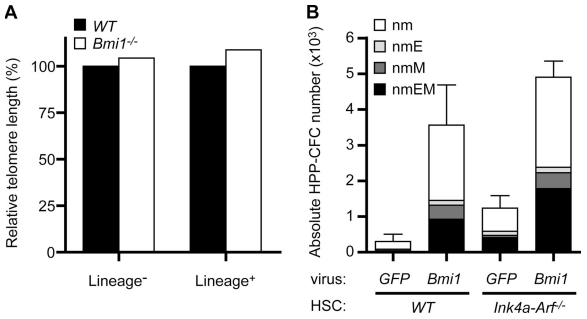

Figure 5. Additional targets for Bmi1 exist other than *Ink4a* and *Arf* genes in the maintenance of HSCs. (A) The relative telomere length of the BM lineage$^-$ and lineage$^+$ cells measured by flow fluorescence in situ hybridization. (B) CD34$^-$KSL cells were transduced with either *GFP* control or *Bmi1* retroviruses and were cultured in the presence of SCF and TPO. At day 10 of culture, colony assays were performed to evaluate the content of HPP-CFCs in culture. GFP$^+$ colonies derived from HPP-CFCs were examined as to their colony types with morphological analysis. The results are shown as the mean ± SD (error bars) of triplicate cultures. Neutrophils, n; macrophages, m; erythroblasts, E; megakaryocytes, M.

HSC self-renewal and multipotential progenitor expansion, although they are largely dispensable in vivo.

Together, all of these observations implicate Bmi1 in both the cell-autonomous and nonautonomous regulation of the HSC system. Similar to BM hematopoiesis, an incomplete recovery of lymphocyte numbers in *Bmi1*$^{-/-}$*Ink4a-Arf*$^{-/-}$ mice could be ascribed to certain defects in the *Bmi1*$^{-/-}$ microenvironment of the spleen and thymus (9, 11). Our findings further unveiled the differential impact of derepressed *Ink4a* and *Arf* on HSCs and their BM microenvironment in *Bmi1*-deficient mice, thus defining *Ink4a* and *Arf* as the major targets for Bmi1 in the maintenance of HSC self-renewal but not of the BM microenvironment.

Finally, Bmi1 has been demonstrated to be essential for the maintenance of leukemic stem cells in a mouse model of acute myelogenous leukemia induced by the *Hoxa9-Meis1* fusion gene (5). It has also been demonstrated that the Rb and p53-dependent cellular senescence plays a critical role to oppose neoplastic transformation triggered by the activation of oncogenic pathways (19). It will be important to investigate whether the up-regulation of Bmi1 contributes to repression of the oncogene-induced senescence pathway in the leukemic transformation and maintenance of the self-renewal capacity of leukemic stem cells.

MATERIALS AND METHODS

Mice. *Bmi1*$^{+/-}$ mice and *Ink4a-Arf*$^{-/-}$ mice (provided by R.A. DePinho, Harvard Medical School, Boston, MA) that had been backcrossed at least eight times onto a C57BL/6 (B6-Ly5.2) background were used. Mice congenic for the Ly5 locus (B6 Ly5.1) were bred and maintained at the Animal Research Center of the Institute of Medical Science (University of Tokyo). All experiments using mice received approval from the Tokyo University Administrative Panel for Animal Care.

Competitive repopulation assay. Hematopoietic cells from B6-Ly5.2 mice were mixed with BM competitor cells (B6-Ly5.1) and were transplanted into B6-Ly5.1 mice irradiated at a dose of 9.5 Gy. Donor cell chimerism in the recipient peripheral blood cells was evaluated as previously described (8). The ability of the *Bmi1*$^{-/-}$ microenvironment to support hematopoiesis was evaluated by transplanting 2×10^6 wild-type BM cells (B6-Ly5.1) into 4-wk-old mutant mice (B6-Ly5.2) sublethally irradiated (*Bmi1*$^{-/-}$ and *Bmi1*$^{-/-}$*Ink4a-Arf*$^{-/-}$ mice, 4.5 Gy; others, 6.5 Gy).

Purification of mouse HSCs and single-cell colony assay. Mouse HSCs (CD34$^-$KSL cells) were purified from BM cells of 8-wk-old mice on a flow cytometry system (FACSVantage; Becton Dickinson) as previously described (8). Single CD34$^-$KSL cells were sorted clonally into 96-well plates containing 200 μl SF-O3 (Sanko Junyaku) supplemented with 5×10^{-5} M 2-β-mercaptoethanol, 2 mM L-glutamine, 10% FBS, 20 ng/ml of mouse SCF, 20 ng/ml of mouse IL-3, 50 ng/ml of human TPO, and 1 unit/ml of human EPO (PeproTech).

Primary BM-derived osteoblast culture and *Bmi1* knockdown. Femurs and tibiae were cut into small pieces after BM cells were fully flushed out. Then, bone fragments were cultured in α-MEM supplemented with 2 mM L-glutamine, 10% FCS, and 5×10^{-5} M 2-β-mercaptoethanol. Suspension cells were removed by replacing the medium. Osteoblastic phenotypes were evaluated by the expression of alkaline phosphatase. A lentivirus vector (CS-H1-shRNA-EF-1α-EGFP) expressing shRNA against mouse *Bmi1* (target sequence TAAAGGATTACTACACGCTAATG) and *Luciferase* was prepared, and the viruses were produced as previously described (23).

RT-PCR. Semiquantitative RT-PCR was performed using normalized cDNA with quantitative PCR using TaqMan rodent GAPDH control reagent (PerkinElmer) as previously described (8).

Quantification of telomere length. Telomere length was quantified on a flow cytometer (FACSCalibur; BD Biosciences) using flow fluorescence in situ hybridization with a Telomere PNA Kit/FITC for flow cytometry (DakoCytomation).

Transduction of CD34$^-$KSL cells. The retrovirus vector pGCDNsam-ires-*EGFP* (provided by M. Onodera, University of Tsukuba, Ibaraki, Japan), the production and concentration of recombinant retrovirus, and the transduction of CD34$^-$KSL cells have been described previously (8). After transduction, the cells were further incubated for 9 d in S-Clone SF-O3 supplemented with 5×10^{-5} M 2-β-mercaptoethanol, 2 mM L-glutamine, 1% FBS, 50 ng/ml SCF, and 50 ng/ml TPO and subjected to in vitro colony assay using a methylcellulose medium (StemCell Technologies Inc.) supplemented with 20 ng/ml of mouse SCF, 20 ng/ml of mouse IL-3, 50 ng/ml of human TPO, and 1 unit/ml of human EPO. GFP$^+$ colony numbers were counted on day 10. Colonies derived from HPP-CFCs (colony diameter of >1 mm) were recovered and morphologically examined. The transduction efficiency was >80% as judged from the GFP expression.

Online supplemental material. Fig. S1 provides data for flow cytometric profiles and frequencies of HSCs in mutant mice. Fig. S2 provides data for the competitive BM repopulating assay using 10 times more test cells than the competitor cells. Fig. S3 provides data for differentiation and the HSC-supporting capacity of osteoblasts in the absence of Bmi1. Fig. S4 provides data for the senescence of *Bmi1* knockdown osteoblasts. Online supplemental material is available at http://www.jem.org/cgi/content/full/jem.20052477/DC1.

We thank Dr. M. Onodera for providing pGCDNsam-ires-EGFP, Dr. R.A. DePinho for *Ink4a*$^{+/-}$ mice, and H. Tsukui and Y. Yamazaki for excellent technical assistance.

This work was supported, in part, by grants from the Ministry of Education, Culture, Sport, Science and Technology of Japan, the Core Research for Evolutional Science and Technology of Japan Science and Technology Corporation, and the Mochida Memorial Foundation for Medical and Pharmaceutical Research.

The authors have no conflicting financial interests.

Submitted: 12 December 2005
Accepted: 10 August 2006

REFERENCES

1. Lund, A.H., and M. van Lohuizen. 2004. Polycomb complexes and silencing mechanisms. *Curr. Opin. Cell Biol.* 16:239–246.
2. Valk-Lingbeek, M.E., S.W.M. Bruggeman, and M. van Lohuizen. 2004. Stem cells and cancer: the polycomb connection. *Cell.* 118:409–418.
3. Iwama, A., H. Oguro, M. Negishi, Y. Kato, and H. Nakauchi. 2005. Epigenetic regulation of hematopoietic stem cell self-renewal by polycomb group genes. *Int. J. Hematol.* 81:294–300.
4. van der Lugt, N.M., J. Domen, K. Linders, M. van Roon, E. Robanus-Maandag, H. te Riele, M. van der Valk, J. Deschamps, M. Sofroniew, M. van Lohuizen, and A. Berns. 1994. Posterior transformation, neurological abnormalities, and severe hematopoietic defects in mice with a targeted deletion of the bmi-1 proto-oncogene. *Genes Dev.* 8:757–769.
5. Lessard, J., and G. Sauvageau. 2003. Bmi-1 determines proliferative capacity of normal and leukemic stem cells. *Nature.* 423:255–260.
6. Molofsky, A.V., R. Pardal, T. Iwashita, I.K. Park, M.F. Clarke, and S.J. Morrison. 2003. Bmi-1 dependence distinguishes neural stem cell self-renewal from progenitor proliferation. *Nature.* 425:962–967.
7. Park, I.K., D. Qian, M. Kiel, M.W. Becker, M. Pihalja, I.L. Weissman, S.J. Morrison, and M.F. Clarke. 2003. Bmi-1 is required for maintenance of adult self-renewing haematopoietic stem cells. *Nature.* 423:302–305.
8. Iwama, A., H. Oguro, M. Negishi, Y. Kato, Y. Morita, H. Tsukui, H. Ema, T. Kamijo, Y. Katoh-Fukui, H. Koseki, et al. 2004. Enhanced self-renewal of hematopoietic stem cells mediated by the polycomb gene product, Bmi-1. *Immunity.* 21:843–851.
9. Jacobs, J.J.L., K. Kieboom, S. Marino, R.A. DePinho, and M. van Lohuizen. 1999. The oncogene and Polycomb-group gene bmi1 regulates proliferation and senescence through the ink4a locus. *Nature.* 397:164–168.
10. Sharpless, N.E., and R.A. DePinho. 1999. The INK4A/ARF locus and its two gene products. *Curr. Opin. Genet. Dev.* 9:22–30.
11. Bruggeman, S.W.M., M.E. Valk-Lingbeek, P.P. van der Stoop, J.J.L. Jacobs, K. Kieboom, E. Tanger, D. Hulsman, C. Leung, Y. Arsenijevic, S. Marino, and M. van Lohuizen. 2005. Ink4a and Arf differentially affect cell proliferation and neural stem cell self-renewal in Bmi1-deficient mice. *Genes Dev.* 19:1438–1443.
12. Molofsky, A.V., S. He, M. Bydon, S.J. Morrison, and R. Pardal. 2005. Bmi-1 promotes neural stem cell self-renewal and neural development but not mouse growth and survival by repressing the p16Ink4a and p19Arf senescence pathways. *Genes Dev.* 19:1432–1437.
13. Osawa, M., K. Hanada, H. Hamada, and H. Nakauchi. 1996. Long-term lymphohematopoietic reconstitution by a single CD34-low/negative hematopoietic stem cells. *Science.* 273:242–245.
14. Takano, H., H. Ema, K. Sudo, and H. Nakauchi. 2004. Asymmetric division and lineage commitment at the level of hematopoietic stem cells: inference from differentiation in daughter cell and granddaughter cell pairs. *J. Exp. Med.* 199:295–302.
15. Calvi, L.M., G.B. Adams, K.W. Weibrecht, J.M. Weber, D.P. Olson, M.C. Knight, R.P. Martin, E. Schipani, P. Divieti, F.R. Bringhurst, et al. 2003. Osteoblastic cells regulate the haematopoietic stem cell niche. *Nature.* 425:841–846.
16. Zhang, J., C. Niu, L. Ye, H. Huang, X. He, W.G. Tong, J. Ross, J. Haug, T. Johnson, J.Q. Feng, et al. 2003. Identification of the haematopoietic stem cell niche and control of the niche size. *Nature.* 425:836–841.
17. Arai, F., A. Hirao, M. Ohmura, H. Sato, S. Matsuoka, K. Takubo, K. Ito, G.Y. Koh, and T. Suda. 2004. Tie2/angiopoietin-1 signaling regulates hematopoietic stem cell quiescence in the bone marrow niche. *Cell.* 118:149–161.
18. Kiel, M.J., O.H. Yilmaz, T. Iwashita, O.H. Yilmaz, C. Terhorst, and S.J. Morrison. 2005. SLAM family receptors distinguish hematopoietic stem and progenitor cells and reveal endothelial niches for stem cells. *Cell.* 121:1109–1121.
19. Campisi, J. 2005. Senescent cells, tumor suppression, and organismal aging: good citizens, bad neighbors. *Cell.* 120:513–522.
20. Allsopp, R.C., G.B. Morin, R. DePinho, C.B. Harley, and I.L. Weissman. 2003. Telomerase is required to slow telomere shortening and extend replicative lifespan of HSCs during serial transplantation. *Blood.* 102:517–520.
21. Allsopp, R.C., G.B. Morin, J.W. Horner, R. DePinho, C.B. Harley, and I.L. Weissman. 2003. Effect of TERT over-expression on the long-term transplantation capacity of hematopoietic stem cells. *Nat. Med.* 9:369–371.
22. Stepanova, L., and B.P. Sorrentino. 2005. A limited role for p16Ink4a and p19Arf in the loss of hematopoietic stem cells during proliferative stress. *Blood.* 106:827–832.
23. Katayama, K., K. Wada, H. Miyoshi, K. Ohashi, M. Tachibana, R. Furuki, H. Mizuguchi, T. Hayakawa, A. Nakajima, T. Kadowaki, et al. 2004. RNA interfering approach for clarifying the PPARgamma pathway using lentiviral vector expressing short hairpin RNA. *FEBS Lett.* 560:178–182.